Int J Clin Exp Med 2015;8(9):14885-14895
www.ijcem.com /ISSN:1940-5901/IJCEM0012030

Original Article

Mitochondrial energy metabolism disorder and apoptosis: a potential mechanism of postoperative ileus

Fan-Feng Chen[1*], Chong-Jun Zhou[1*], Cheng-Le Zhuang[1], Dong-Dong Huang[1], Jin-Xiao Lu[1], Xian Shen[1], Xiao-Lei Chen[1], Zhen Yu[1,2]

[1]Department of Gastrointestinal Surgery, The First Affiliated Hospital of Wenzhou Medical University, Wenzhou 325000, China; [2]Department of Surgery, Shanghai Tenth People's Hospital Affiliated to TongJi University, Shanghai 200072, China. [*]Equal contributors.

Received June 28, 2015; Accepted September 10, 2015; Epub September 15, 2015; Published September 30, 2015

Abstract: Aim: To explore whether mitochondrial energy metabolism disorder and apoptosis of smooth muscle cells in intestinal muscularis are participated in pathogenesis of postoperative ileus (POI). Methods: Rats were randomized into three groups: naive controls (NC) group, sham controls (SC) group and intestinal manipulation (IM) group. Gastrointestinal transits were analyzed. Reactive oxygen species (ROS), malondialdehyde (MDA) and adenosine triphosphatases (ATPases) activity in intestinal muscularis were determined. The levels of aldehyde dehydrogenase 2 (ALDH2), Bcl-2 and Bax in intestinal muscularis were measured by real-time PCR assays and western blot analysis. The levels of ATP, ADP and AMP in intestinal muscularis were determined by high performance liquid chromatography. Transmission electron microscopic was used to observe ultrastructure of smooth muscle cells and mitochondria in intestinal muscularis. Results: Delayed gastrointestinal transitoccurred only in IM groups. After IM, increased levels of ROS and MDA were observed in intestinal muscularis. In IM groups, we also observed decreased levels of ALDH2 and Bcl-2/Bax ratio. The levels of ATP and ADP were decreased and level of AMP was increased in IM groups. The activity of ATPases was decreased in IM groups. Abnormal morphological architecture of smooth muscle cells and mitochondria were found in intestinal muscularis of IM groups. Conclusion: Our results suggest that mitochondrial energy metabolism disorder and apoptosis of smooth muscle cells in intestinal muscularis may participate in the development of POI.

Keywords: Postoperative ileus, oxidative stress, mitochondria, energy metabolism, apoptosis

Introduction

Postoperative ileus (POI) is an iatrogenic condition that occurs following almost every abdominal surgery characterized by generalized hypomotility of the gastrointestinal tract, the clinical manifestations include abdominal distension, nausea, vomiting and the inability to pass stools or tolerate a solid diet [1, 2]. In addition to the discomfort experiences of patients, POI is also leads to increased morbidity, prolonged hospitalization and, therefore, increased total treatment cost [3]. Neural sympathetic inhibitory reflexes and intestinal inflammatory responses are generally considered to participate in the development of POI [4, 5]. Currently, numerous pharmacologic interventions have been used in an attempt to shorten the length of POI after abdominal surgery, such as prokinetic drugs and newer attempts to use anti-inflammatory agents. But the therapeutic effects of these treatments were unsatisfactory [6-8]. The reason for limited success to treat POI may be that the aetiology of POI is multifactorial and underlying mechanisms of POI are still unclear.

Besides these well reported mechanisms of POI, other mechanisms, such as oxidative stress, are believed to be related to gastrointestinal dysmotility after abdominal surgery. De Backer et al. have detected a markedly increased oxidative stress levels in intestinal muscularis in POI model of mice [9]. But it still lacks an in-depth research on oxidative stress in POI model of animals. Oxidative stress describes an imbalance between antioxidant defenses and the production of ROS [10]. Previous studies

have demonstrated that oxidative stress mediated mitochondrial dysfunction and nuclear DNA damage, can contribute to a labile cell redox state, leading to the promotion of cell apoptosis [11-13]. Mitochondria have a fundamental role in the maintenance of the normal structure and function of tissues. In addition, mitochondria are also the most important energy sources, efficiently generating ATP [14, 15]. A decline in mitochondrial function impaired the normal regulation of redox state, energy metabolism, apoptosis and intracellular signaling [16, 17]. Besides, previous studies have demonstrated that some mitochondrially located enzymes, such as ALDH2, are involved in antioxidant defense [18, 19].

However, the role of mitochondrial energy metabolism disorder and apoptosis of smooth muscle cells in intestinal muscularis in POI has not been investigated, which we hypothesized to be participated in the pathogenesis of POI.

Materials and methods

Animal

Male Sprague-Dawley rats (weighing 210-230 g) were provided by Vital River Laboratory Animal Technology Co., Ltd. (Beijing, China). All the animals were maintained under specific-pathogen-free conditions, at acontrolled temperature (21±1°C), humidity (50%±5%) and 12-h light and 12-h dark cycles (light, 08:00-20:00 h; darkness, 20:00-08:00 h) with a free access to standard laboratory rat chow and tap water. All the animals were allowed a minimum of oneweek acclimatization before study. This animal protocol was reviewed and approved by the Institutional Animal Committee of Wenzhou Medical University. All the experiments were performed according to the National Institutes of Health Guidelines on the use of laboratory animals. All the experiments were conducted in accordance with "Guide for the Care and Use of Laboratory Animals". All efforts were made to minimize the number of animals and their suffering.

Experimental groups and operative procedures

Age-matched rats were randomized assigned to 3 experimental groups: Non-operated rats without anesthesia served as naive controls (NC; n=8) group, rats undergoing surgical anesthesia and manipulation of the small intestine served as intestinal manipulation (IM; n=32) group, rats undergoing the above-mentioned procedure without intestinal exteriorization and manipulation served as sham controls (SC; n=32) group. The small intestine was subjected to a standardized degree of surgical manipulation as described previously [20]. Briefly, after the rats were anesthetized, a 3 cm midline incision was made into the peritoneal cavity. The entire small intestine was exteriorized on a moist gauze padand the small intestine from the ligament of Treitz to the ileocecal junction was gently manipulated in its entirety by an aboral compression of the gut lumen using two sterile, moist cotton applicators, which lasted-for 15 minutes. Touching the mesentery was strictly avoided. Thereafter, the intestine was returned into the abdominal cavity and the incision was closed using two-layer continuous sutures. After closure, Animals recovered from anesthesia in a heated recovery cage where they had free access to water and rat chow within 12 hours.

Gastrointestinal transit measurements

Gastrointestinal transit was measured 24 h postoperatively by evaluating the intestinal distribution of orally gavaged fluorescein isothiocyanate (FITC)-labeled dextran [21]. Food pellets were removed from the cage 3 h before sacrifice. Rats were administered 200 μl FITC-dextran (70,000 Da; Invitrogen, Paisley, UK) dissolved in 0.9% saline (6.25 mg/mL) via oral gavage and water was removed from the cage. Ninety minutes after administration, the animal was sacrificed, the abdomen was opened and the gastrointestinal part was isolated, the stomach and intestine were separated as a single stomach segment (Sto), ten small intestine segments (SI1-SI10), a single cecum segment (Cec) and three colon segments (Co1-Co3). The contents of each segment were collected and assayed for the presence of fluorescent label (Synergy HT, BioTek Instruments Inc., VT, USA; excitation wavelength: 485 nm, emission wavelength: 528 nm) for quantification of the fluorescent signal in each bowel segment. GI transit was calculated as the geometric center (GC) of distribution of fluorescence marker using this formula: (GC): $\sum$ (percent of total fluorescent signal in each segment) × (segment number)/100 for quantitative statistical comparison among experimental groups.

Table 1. The primer sequences used for RT-PCR

Gene	Primer	Sequence	Product (bp)
ALDH2	Sense	5'-TCACAGGTTCCACTGAGGTTG-3'	106
	Antisense	5'-ATGATGATATTGGGGCTCTTTCC-3'	
Bcl-2	Sense	5'-ACTTCTCTCGTCGCTACCGTCG-3'	111
	Antisense	5'-CCCTGAAGAGTTCCTCCACCACC-3'	
Bax	Sense	5'-GATGGCCTCCTTTCCTACTTCGG-3'	185
	Antisense	5'-CCTTTCCCCGTTCCCCATTCAT-3'	
β-actin	Sense	5'-TCACCAACTGGGACGATATG-3'	119
	Antisense	5'-GTTGGCCTTAGGGTTCAGAG-3'	

ALDH2, aldehyde dehydrogenase 2; Bcl-2, B-cell lymphoma 2; Bax, Bcl-2-associated X protein.

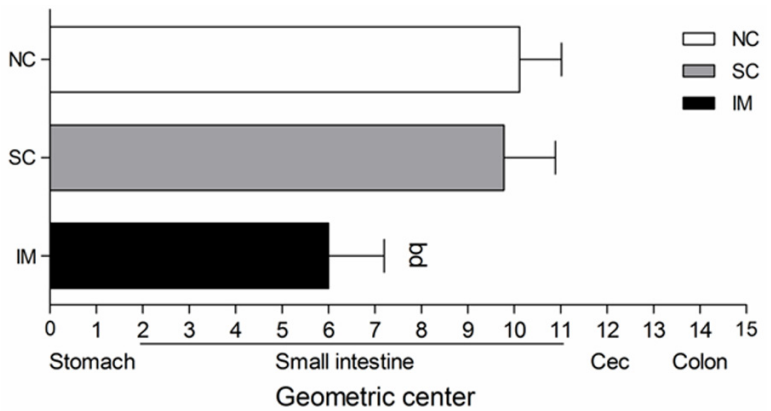

Figure 1. Mean calculated geometric centre for the distribution of FITC-labeled dextran (70 kDa) along the gastrointestinal tract. Values are expressed as the mean ± S.D. [b]*P*<0.01 vs NC; [d]*P*<0.01 vs SC. NC, naive controls; SC, sham controls; IM, intestinal manipulation; Cec, cecum.

Whole mount preparation

At the time of sacrifice (in the SC and IM groups, animals were sacrificed and tissue was harvested at four different time points: 3 h, 6 h, 12 h, and 24 h), rats were anesthetized by intraperitoneal injection of a lethal dose of pentobarbital sodium, abdomen was opened by a midline laparotomy and samples were collected from the 7th segment of the small intestine (SI7). Mesenteric attachment was removed and the segments were cut open along the mesentery border, fecal content was washed out in ice-cold modified Krebs solution, and segments were fixed with 100% ethanol for 10 minutes, transferred to ice-cold modified Krebs solution and pinned flat in a glass-dish. Mucosa and submucosa were carefully removed, musculari-sexterna isolates were snap-frozen in liquid nitrogen and stored at -80°C.

Determination of protein concentration

Protein concentrations were determined using a bicinchoninic acid protein assay kit (Pierce, Rockford, IL, USA).

Real-time quantitative polymerase chain reaction (PCR) assays

Real-time quantitative PCR were performed for quantitate expression of the ALDH2, Bcl-2 and Bax mRNA levels. The total RNA was extracted using TriPure isolation reagent (Roche Diagnostics GmbH, Mannheim, Germany) according to the manufacturer's protocol and the integrity of RNA was identified by the method agarose gel electrophoresis. RNA purity and concentration were assessed by UV spectrophotometry (2.0>A260: A280>1.8). Then 1 μl total RNA was reverse transcribed to 50 μl cDNA with reverse-transcription (RT) kit (TOYOBO Co., Ltd., Japan). Real-time quantitative PCR-experiments were performed using ABI Prism 7500HT (Applied Biosystems, Carlsbad, CA, U.S.A.) with SYBR Green RT-PCR Master Mix (TOYOBO Co., Ltd.). The reaction parameters were incubation at 95°C for 3 min, followed by 40 cycles of 95°C for 15 s, 60°C for 15 s, 72°C for 45 s and then melting curve was used. All reactions were performed in triplicates and normalized using β-actin as an endogenous control gene. The expression levels of mRNA were expressed as relative to control and were compared as fold change using the comparative Ct method described previously [22]. The sense sequence and the anti-sense sequence of each gene were shown in **Table 1**.

Western blot analysis

Western blots were performed on proteins from intestinal muscularis tissue homogenates, which was homogenized in RIPA lysis buffer (Beyotime Biotechnology, China). Proteins sam-

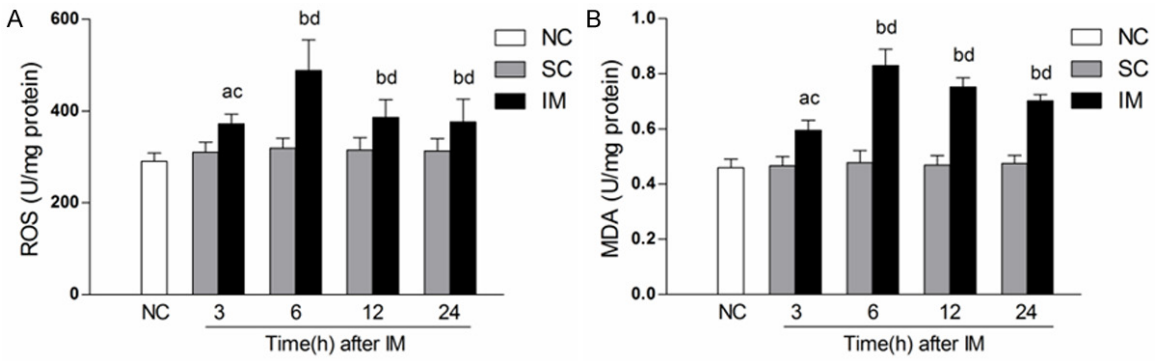

Figure 2. Oxidative stress levels in intestinal muscularis. A. Formation of ROS in intestinal muscularis. B. MDA content in intestinal muscularis. MDA, malondialdehyde; ROS, reactive oxygen species; Values are expressed as the mean ± S.D. [a]*P*< 0.05, [b]*P*<0.01 vs NC; [c]*P*<0.05, [d]*P*<0.01 vs SC. NC, naive controls; SC, sham controls; IM, intestinal manipulation.

Table 2. Myenteric energy metabolism levels

Groups	Time	ATP (nmol/mg)	ADP (nmol/mg)	AMP (nmol/mg)
NC	-	10.88±1.33	5.02±0.49	2.75±0.49
SC	3 h	9.91±1.23	5.13±0.44	3.02±0.66
	6 h	10.74±1.19	4.84±0.36	2.85±0.73
	12 h	10.43±1.27	4.97±0.40	2.75±0.77
	24 h	9.62±1.50	5.08±0.69	2.98±0.68
IM	3 h	9.71±1.47	4.79±0.53	3.07±0.55
	6 h	7.56±1.64[b,d]	3.64±0.49[b,d]	3.86±0.43[b,d]
	12 h	3.95±1.04[b,d]	2.33±0.38[b,d]	4.78±0.58[b,d]
	24 h	4.56±1.56[b,d]	3.01±0.71[b,d]	4.14±0.56[b,d]

The results showed content of ATP, ADP, and AMP in intestinal muscularis. ATP, Adenosine triphosphate; ADP, Adenosine diphosphate; AMP, Adenosine monophosphate; Values are expressed as the mean ± S.D. [b]*P*<0.01 vs NC; [d]*P*<0.01 vs SC. NC, naive controls; SC, sham controls; IM, intestinal manipulation.

ples (30 μg) were separated on 10% sodium dodecyl sulfate-polyacrylamide gel electrophoresis (SDS-PAGE) by electrophoresis performed according to standard procedures. After the electrophoresis, the gel was separated from the glass plates and the proteins were electrotransferred onto a polyvinylidenedifluoride (PVDF) membrane (Millipore, Bedford, MA, U.S.A.) in a wet transfer system (Bio-Rad, U.S.A.). The membranes were blocked with 5.0% skim milk in TBST (TBS containing 0.05% Tween 20) at room temperature for 1 h and subsequently incubated overnight at 4°C with the primary antibody. The primary antibodies were rabbit anti-ALDH2 monoclonal antibody (1: 1000; Abcamplc, Cambridge, U.K.), rabbit anti-Bcl-2 polyclonal antibody (1:100; Abcamplc, Cambridge, U.K.), and rabbit anti-Bax monoclonal antibody (1:1000, Santa Cruz, USA). β-actin (rabbit anti-β-actin primary antibody; 1:3000; from Goodhere Biotechnology Co., Ltd., Hangzhou, China) protein expression was used as an internal control. After four washings with TBST over 5 min, the membranes were incubated at room temperature for 1 h with the appropriate secondary antibody (HRP-conjugated anti-IgG antibody, Biosharp, China; 1:5000). Immunoreactive bands were captured on autoradiography film (Blue X-Ray Film, Phoenix Research, Candler, NC, USA) and the resulting labeled bands were quantified with Quantity One software 4.6.2 (Bio-Rad, Hercules, CA, USA). The quantification of proteins was performed by calculating the density of each individual band sample and was compared as fold change to internal control.

Measurement of myenteric malondialdehyde (MDA)

To measure the level of MDA (a presumptive marker of oxidant-mediated lipid peroxidation), a commercial available kit purchased from Nanjing Jiancheng Bioengineering institute (Nanjing, China) was used. Samples were homogenized in ice-cold phosphate-buffered saline (PBS) and centrifuged at 2500 rpm/min for 15 min at 4°C. The MDA content was measured spectrophotometrically at wavelengths of 532 nm using a Varioskan Flash (Thermo Fisher Scientific Waltham, MA, USA).

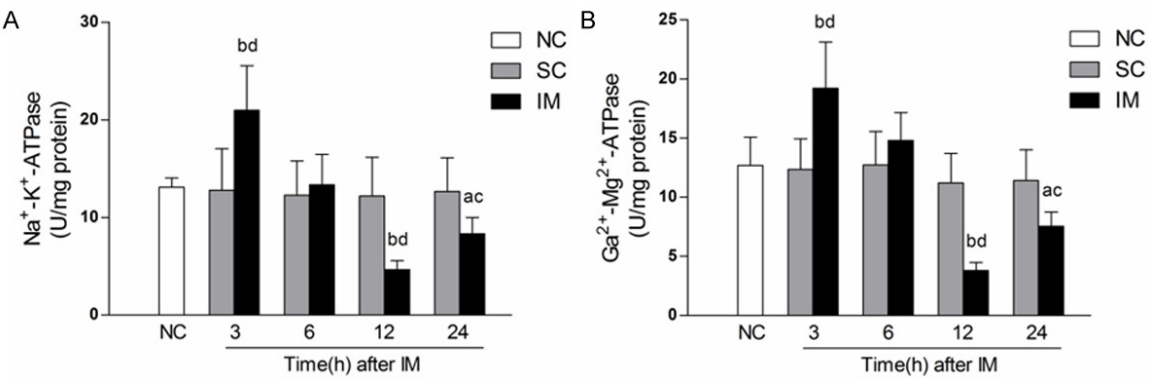

Figure 3. ATPases activity in intestinal muscularis. A. The activity of Na^+-K^+-ATPase in intestinal muscularis; B. The activity of Ca^{2+}-Mg^{2+}-ATPase in intestinal muscularis. Values are expressed as the mean ± S.D. [a]$P<0.05$, [b]$P<0.01$ vs NC; [c]$P<0.05$, [d]$P<0.01$ vs SC. NC, naive controls; SC, sham controls; IM, intestinal manipulation.

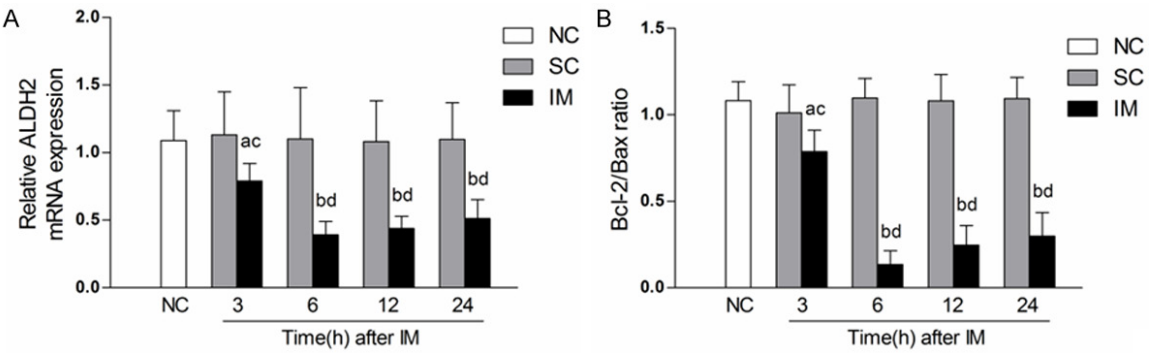

Figure 4. The levels of mRNA expression of ALDH2, Bcl-2 and Bax in intestinal muscularis. β-actin was used as an internal control. ALDH2, aldehyde dehydrogenase 2; Bcl-2, B-cell lymphoma 2; Bax, Bcl-2-associated X protein. Values are expressed as the mean ± S.D. [a]$P<0.05$, [b]$P<0.01$ vs NC; [c]$P<0.05$, [d]$P<0.01$ vs SC. NC, naive controls; SC, sham controls; IM, intestinal manipulation.

Measurement of myenteric reactive oxygen species (ROS)

To measure the level of intracellular ROS, the fluorescent probe 2'7'-dichlorofluorescin diacetate (DCFH-DA) (Nanjing Jiancheng Bioengineering institute, Nanjing, China) was used. Samples were homogenized in ice-cold phosphate-buffered saline (PBS) and centrifuged at 1000× g for 10 min at 4°C. Supernatants were incubated with 1 mmol/L DCFH-DA for 30 min at 37°C in the dark. The fluorescence was measured using a Varioskan Flash (Thermo Fisher Scientific Waltham, MA, USA) at an excitation wavelength of 502 nm and an emission wavelength of 530 nm. Final results of ROS were normalized to protein concentration.

Measurement of myenteric ATP synthases activity

The activity of Na^+-K^+-ATPase and Ca^{2+}-Mg^{2+}-ATPase were measured using a commercial available kit purchased from Nanjing Jiancheng Bioengineering institute (Nanjing, China). The optical density (OD) was measured using a Varioskan Flash (Thermo Fisher Scientific Waltham, MA, USA) at a wavelength of 532 nm. Final results of Na^+-K^+-ATPase and Ca^{2+}-Mg^{2+}-ATPase activity were normalized to protein concentration.

High performance liquid chromatography (HPLC)

Intestinal muscularis samples were processed with 5% perchloric acid for removing the impurities and then centrifuged at 4000 rpm/min at 4°C for 15 min. The supernatant solutions were adjusted to pH 6.5 with 2 mol/LKOH, and then centrifuged at 4000 rpm/min at 4°C for 15 min again. The supernatant solutions were measured for the concentrations of adenosine triphosphate (ATP), adenosine diphosphate (ADP) and adenosine monophosphate (AMP) using the HPLC-fluorescence detection system

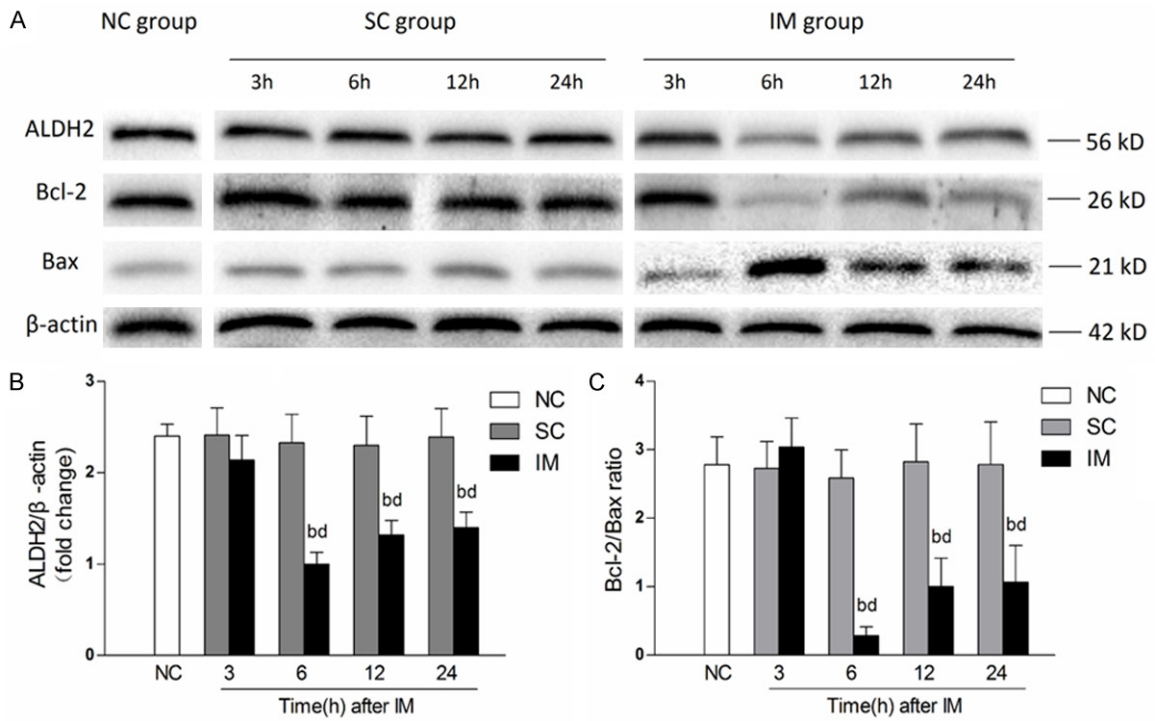

Figure 5. The levels of protein expression of ALDH2, Bcl-2 and Bax in intestinal muscularis. A. Representative western blot; B. Quantitative analysis of the ALDH2/β-actin protein expression ratios in intestinal muscularis; C. Quantitative analysis of the Bcl-2/Bax protein expression ratios in intestinal muscularis. β-actin was used as an internal control. ALDH2, aldehyde dehydrogenase 2; Bcl-2, B-cell lymphoma 2; Bax, Bcl-2-associated X protein. Values are expressed as the mean ± S.D. [b]*P*<0.01 vsNC; [d]*P*<0.01 vs SC. NC, naive controls; SC, sham controls; IM, intestinal manipulation.

(Agilent 1260 Infinity, U.S.A.) with a Hyspersil C18 column (250 mm×4.6 mm i.d., 5 mm particle size, from Elite Analytical Instrument Co., Ltd., Dalian, China). A variable wave length UV detector (Model HP 1050) monitored the absorbance of the eluents at 254 nm. Detector signals were recorded and integrated by Chemstation HP software. Buffers were prepared with ultrapure water and degassed by sonication before use. Buffer A consisted of 12 mmol/L Na_2HPO_4 and 88 mmol/L NaH_2PO_4. The mobile phase consisted of Buffer A with 1% (v/v) acetonitrile. The flow rate was maintained at 1.0 mL/min. The fluorescence excitation and emission wavelengths and the preparation of standard working solutions were described previously [23]. ATP, ADP and AMP were purchased from Sigma (St. Louis, MO, U.S.A.). Their concentrations were determined from ratios of their peak areas to standards separately.

Transmission electron microscopic (TEM) analysis

To reflect the ultrastructural changes of smooth muscle cells and mitochondria in intestinal muscularis, an ultrastructural TEM analysis were performed on 24 h postoperatively (the time point gastrointestinal transits were analyzed). After dissection, small pieces of the intestinal samples were cut into 1 mm^3 and immediately fixed in 2.5% glutaraldehyde at 4°C overnight. Samples were then post-fixed in 1% osmium tetroxide for 1 h followed by dehydrated through an ascending acetone series (50%, 70%, 90%, 95%, 100% and 100% again, respectively), every treating for 10 min. Specimens were embedded in a acetone and epoxy resin mixture for 72 h at 40°C and for 24 h at 60°C. Semiultrathin sections were stained with toluidine blue. Ultra-thin sections were fabricated and observed by TEM (H-7500, HITACHI, Tokyo, Japan). The images collection and statistical analysis were completed.

Statistical analysis

All the data are expressed as mean ± standard deviation (S.D.). The significance of the mean difference was determined by one-way ANOVA, followed by post-hoc tests (using Least Significant Difference test, LSD-t) for multi-group-

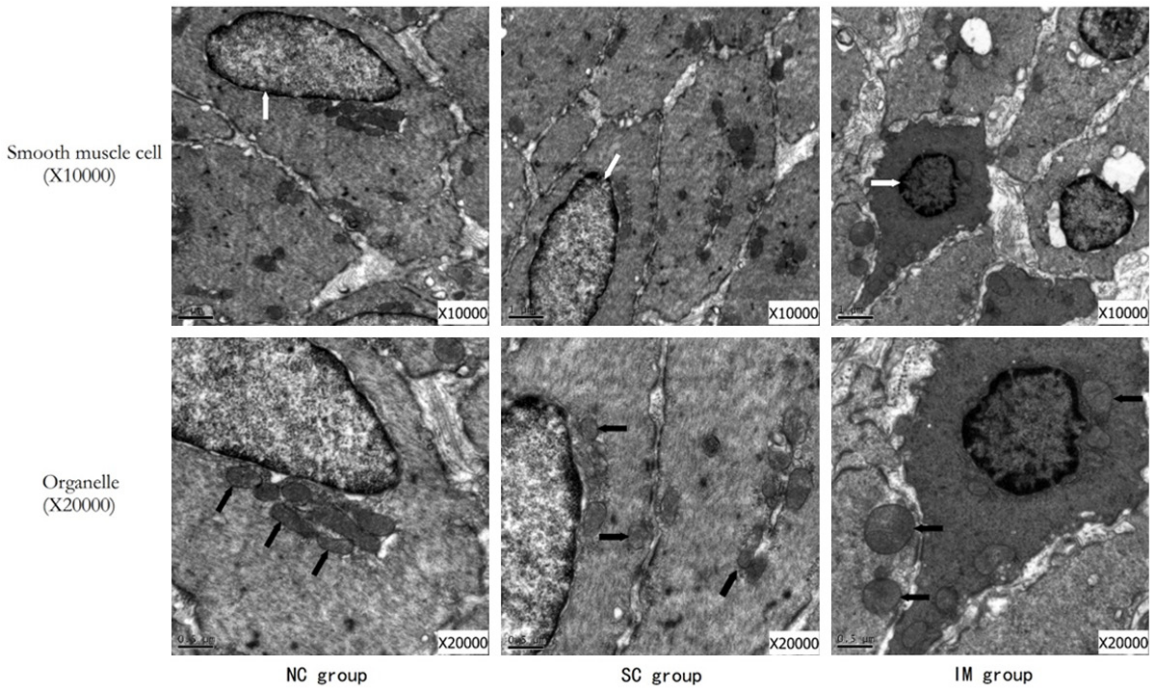

Figure 6. Representative photographs of TEM of smooth muscle cells and mitochondria in intestinal muscularis (×10000 and ×20000). Cell nuclear of smooth muscle cells indicated by black arrow; Mitochondria indicated by white arrow. NC, naive controls; SC, sham controls; IM, intestinal manipulation.

comparisons. Differences between groups with $P<0.05$ were considered statistically significant. Statistical analyses were performed using the IBM SPSS Statistics for Windows, Version 20.0.

Result

Gastrointestinal transit

The distribution histogram shows a significant delay in transit of the FITC-labeled marker measured in IM groups ($P<0.01$; **Figure 1**). In contrast, sham operation had no effect on gastrointestinal transit.

Myenteric oxidative stress levels

When compared to NC and SC groups, the formation of ROS (**Figure 2A**) and content of MDA (**Figure 2B**) in intestinal muscularis were increased in IM groups with the greatest values at 6 h ($P<0.01$). In contrast, sham controls did not cause any changes in ROS and MDA after sham operation.

Myenteric energy metabolism levels

The levels of ATP, ADP and AMP are shown in **Table 2**. When compared to NC and SC groups, there was a tendency of deceased concentrations of ATP and ADP and increased concentrations of AMP in the IM groups with the most pronounced effect at 12 h ($P< 0.01$). In addition, sham operation did not cause any changes in the levels of ATP, ADP and AMP.

Changes in ATPases activity

When compared to NC and SC groups, after a significant rise at 3 h, the activity of Na^+-K^+-ATPase (**Figure 3A**) and Ca^{2+}-Mg^{2+}-ATPase (**Figure 3B**) were soon decreased in IM groups with the most pronounced effect at 12 h ($P<0.01$). In contrast, sham controls did not cause any changes in the activity of Na^+-K^+-ATPase and Ca^{2+}-Mg^{2+}-ATPase after sham operation.

Myentericapoptosis levels

The results of RT-PCR and western blot analysis revealed that, compared with that of the NC and SC groups, the Bcl-2/Bax ratios at the mRNA (**Figure 4B**) and protein (**Figure 5C**) levels were both decreased in IM groups at 6 h, 12 h and 24 h with the most pronounced effect at 6 h ($P<0.01$). In contrast, sham controls did not cause any changes in the Bcl-2/Bax ratios after sham operation.

Changes in the expression levels of ALDH2

The mRNA and protein expressions of ALDH2 are shown in **Figures 4A** and **5B**, respectively. The western blot analysis and RT-PCR assays revealed that, compared with that of the NC and SC groups, the ratios of ALDH2/β-actin at the mRNA and proteins level were both decreased in IM groups at 6 h, 12 h and 24 h with the most pronounced effect at 6 h ($P<0.01$). In contrast, sham operation had no effect on mRNA and protein expressions of ALDH2.

Ultrastructural changesin intestinal muscularis

Figure 6 shows the ultrastructure micrographs of smooth muscle cellsand mitochondria in intestinal muscularis in three groups. The electron micrographs showed normal morphological architecture of smooth muscle cells and mitochondria in intestinal muscularis from NC and SC groups. Nuclear shrinkage and chromatin condensation of smooth muscle cells, swelling and rupturing of the mitochondria with distorted cristae can be seen in IM groups.

Discussion

POI after abdominal surgery has traditionally been accepted as an inevitable event. Clinically, it is characterized by a transient inhibition of coordinated motility of the gastrointestinal tract after abdominal surgery and leads to increased morbidity and prolonged hospitalization [24]. Currently, manipulation of the small intestine is widely used as a preclinical model of POI [20]. The aetiology of POI is multifactorial, but insights into the pathogenesis of POI, neurogenic, inflammatory and inflammatory-neuronal interactive mechanisms are generally considered to induce POI [25]. However, the exact mechanism of POI is still unknown. As far as our knowledge, this is the first study reporting the mitochondrial energy metabolism disorder and apoptosis of smooth muscle cells in intestinal muscularisthat might participate in the pathophysiology of POI in a rat model induced bymanipulation of the small intestine.

De Backer et al. have detected an early and transient increase of oxidative stress in the immediate postoperative phase, which further increased until the end of the experiment [9]. Oxidative stress describes an imbalance between antioxidant defenses and the production of ROS, which at high levels triggers lipid peroxidation [26, 27]. Mitochondria have been suggested to be the key sources of ROS [28]. In congruence with earlier studies, we observed an increase in formation of ROS and content of MDA in IM groups. Not only producing ROS, mitochondria are also the targets of oxidative stress. Prior to the present study, it had already been reported that disorganization of the ultrastructure in mitochondria accompanied the aggravation of oxidative stress during experimental pulmonary carcinogenesis [29]. In our study, the electron micrographs shows mitochondrial swelling with distorted cristae indicating mitochondrial degeneration from IM groups compared with mitochondria from NC and SC groups. In addition, cell atrophy, particularly nuclear shrinkage and chromatin condensation of smooth muscle cells in IM groups were also observed, which suggested that parts of smooth muscle cells were in early stage of apoptosis. The atypia was degenerative and not observed in NC and SC groups. Those degenerative changes in ultrastructure of smooth muscle cells and mitochondria in intestinal muscularis may be associated with gastrointestinal motility impairment.

After observation of the degenerative changes in ultrastructure, we further researched the functional impairment of mitochondria in POI model rats. Mitochondria are the most important cellular organelle that generates ATP and supplies cells with energy [30]. However, mitochondria energy metabolism is extremely sensitive to impairment by ROS. The findings of the present study showed the mitochondrial formation of ATP was declined in IM groups compared with those in NC and SC groups, which demonstrated an aberrant in energy metabolism in intestinal muscularis of POI model rats. Furthermore, energy metabolism includes anabolism and catabolism with many biological enzymes involved in [31]. Na^+/K^+-ATPase and Ca^{2+}/Mg^{2+}-ATPase are two ATP-hydrolyzing enzymes, which have an ability to hydrolyze ATP to supply direct free energy [32]. ATP-hydrolyzing enzyme plays an important role in maintaining physiologic functions of the energy conversion, material transport, and information transmission [33]. As the results showed, in parallel with changes in ATP, activity of Na^+/K^+-ATPase and Ca^{2+}/Mg^{2+}-ATPase were both significantly decreased in IM groups.

Apoptosis of intestinal smooth muscle cells have been observed by TEM analysis. We further investigated the underlying apoptosis pathways that are activated in POI model rats. Previous study has indicated that oxidative stress leads to a sharp rise in intracellular ROS production by mitochondria and activation of mitochondrial apoptotic pathways in intestinal epithelial cells [12]. Cell apoptosis of mitochondria pathway is mediated by Bcl-2 family proteins. In brief, in the mitochondrial pathway, inactivating of Bcl-2 and Bcl-XL promotes the opening of mitochondrial permeability transition pore (MPTP), subsequently reduces mitochondrial membrane potentialand increasing intracellular Ca^{2+} concentration, finally leading to Cyt C release [34]. The balance in the expression levels of the anti-apoptotic Bcl-2 and the pro-apoptotic Bax proteins has a major role in the regulation of apoptotic cell death [35, 36]. The Bcl-2/Bax ratio represents the extent of apoptosis [37]. In the present study, it was shown that in the IM groups, Bcl-2/Bax ratio in intestinal muscularis was significantly decreased. These results suggesting that the mitochondrial apoptosis pathway activated maycontribute to cell apoptosis in POI model of rats.

Mitochondrially located enzymes are essential to antioxidant defense and maintenance of mitochondria function [19]. Mitochondrial ALDH2 participates in one of the major metabolic pathways for the removal of acetaldehyde and other toxic aldehydes [38], thereby playing a part in protecting cells against the oxidative stress [39]. Previous study has indicated that ALDH2 has a great importance in chronic alcohol ingestion-induced hepatic damage, as the overexpressions of ALDH2 effectively ameliorate alcohol-induced hepatic apoptosis [40]. Ren et al. suggested that transgenic overexpression of ALDH2 rescues chronic alcoholism-elicited cerebral injury [41]. When ethanol was administered in order to induce ALDH2 activity in diabetic rats, the levels of oxidative stress and the occurrence of apoptosis were ameliorated [42, 43]. In present study we found that the mRNA and protein expressions of ALDH2 were both decreased in groups at 6 h, 12 h, and 24 h in IM groups. It was interesting that, the decreased ALDH2 level was accompanied by a decreased level of Bcl-2/Bax ratio in intestinal muscularis. Our results suggested that the decreased expression levels of the ALDH2 may contribute to the occurrence of apoptosis of smooth muscle cells. Although ALDH2 is essential for cell survival, the mechanism of how decreased ALDH2 expression levels leads to apoptosis of smooth muscle cells remains to be fully elucidated.

Conclusion

In summary, our study provided evidences that mitochondrial energy metabolism disorder and apoptosis of smooth muscle cells in intestinal muscularis are involved in pathophysiological mechanisms of POI, at least in part, relevant to the mitochondrial ALDH2 activity impairment by ROS. To our knowledge, this is the first report that reveals the relationships between mitochondrial events and gastrointestinal dysmotility in POI model rats. In addition to the currently accepted mechanisms of POI, mitochondrial energy metabolism disorder and apoptosis of smooth muscle cells should be noticed as a new potential pathogenesis and may show a new target to shorten the duration of postoperative gastrointestinal ileus pharmacologically.

Acknowledgements

This work was supported by the National Natural Science Foundation of China (No. 811-71857).

Disclosure of conflict of interest

None.

Address correspondence to: Zhen Yu and Xiao-Lei Chen, Department of Gastrointestinal Surgery, The First Affiliated Hospital, Wenzhou Medical University, 2 Fuxue Lane, Wenzhou 325000, Zhejiang, China. Tel: +0086-0577-55579442; Fax: +0086-0577-88069555; E-mail: yuzhen0577@gmail.com (ZY); chenxiaolei0577@126.com (XLC)

References

[1] Holte K and Kehlet H. Postoperative ileus: a preventable event. Br J Surg 2000; 87: 1480-1493.

[2] Mueller MH, Karpitschka M, Gao Z, Mittler S, Kasparek MS, Renz B, Sibaev A, Glatzle J, Li Y and Kreis ME. Vagal innervation and early postoperative ileus in mice. J Gastrointest Surg 2011; 15: 891-900; discussion 900-891.

[3] Kraft MD. Methylnaltrexone, a new peripherally acting mu-opioid receptor antagonist being evaluated for the treatment of postoperative ileus. Expert Opin Investig Drugs 2008; 17: 1365-1377.
[4] Bragg D, El-Sharkawy AM, Psaltis E, Maxwell-Armstrong CA and Lobo DN. Postoperative ileus: Recent developments in pathophysiology and management. Clin Nutr 2015; 34: 367-376.
[5] Senagore AJ. Pathogenesis and clinical and economic consequences of postoperative ileus. Clin Exp Gastroenterol 2010; 3: 87-89.
[6] Johnson MD and Walsh RM. Current therapies to shorten postoperative ileus. Cleve Clin J Med 2009; 76: 641-648.
[7] Kehlet H. Postoperative ileus--an update on preventive techniques. Nat Clin Pract Gastroenterol Hepatol 2008; 5: 552-558.
[8] Klohnen A. New perspectives in postoperative complications after abdominal surgery. Vet Clin North Am Equine Pract 2009; 25: 341-350.
[9] De Backer O, Elinck E, Blanckaert B, Leybaert L, Motterlini R and Lefebvre RA. Water-soluble CO-releasing molecules reduce the development of postoperative ileus via modulation of MAPK/HO-1 signalling and reduction of oxidative stress. Gut 2009; 58: 347-356.
[10] Rosenfeldt F, Wilson M, Lee G, Kure C, Ou R, Braun L and de Haan J. Oxidative stress in surgery in an ageing population: pathophysiology and therapy. Exp Gerontol 2013; 48: 45-54.
[11] Ahmad MK, Khan AA, Ali SN and Mahmood R. Chemoprotective effect of taurine on potassium bromate-induced DNA damage, DNA-protein cross-linking and oxidative stress in rat intestine. PLoS One 2015; 10: e0119137.
[12] Baregamian N, Song J, Papaconstantinou J, Hawkins HK, Evers BM and Chung DH. Intestinal mitochondrial apoptotic signaling is activated during oxidative stress. Pediatr Surg Int 2011; 27: 871-877.
[13] Chakrabarti S, Poidevin M and Lemaitre B. The Drosophila MAPK p38c regulates oxidative stress and lipid homeostasis in the intestine. PLoS Genet 2014; 10: e1004659.
[14] Elamin E, Masclee A, Troost F, Dekker J and Jonkers D. Cytotoxicity and metabolic stress induced by acetaldehyde in human intestinal LS174T goblet-like cells. Am J Physiol Gastrointest Liver Physiol 2014; 307: G286-294.
[15] Szabo C, Ransy C, Modis K, Andriamihaja M, Murghes B, Coletta C, Olah G, Yanagi K and Bouillaud F. Regulation of mitochondrial bioenergetic function by hydrogen sulfide. Part I. Biochemical and physiological mechanisms. Br J Pharmacol 2014; 171: 2099-2122.
[16] Picard M, Taivassalo T, Gouspillou G and Hepple RT. Mitochondria: isolation, structure and function. J Physiol 2011; 589: 4413-4421.
[17] Ryan MT and Hoogenraad NJ. Mitochondrial-nuclear communications. Annu Rev Biochem 2007; 76: 701-722.
[18] Huang XP, Tan H, Chen BY and Deng CQ. Combination of total astragalus extract and total Panax notoginseng saponins strengthened the protective effects on brain damage through improving energy metabolism and inhibiting apoptosis after cerebral ischemia-reperfusion in mice. Chin J Integr Med 2015; [Epub ahead of print].
[19] Wenzel P, Schuhmacher S, Kienhofer J, Muller J, Hortmann M, Oelze M, Schulz E, Treiber N, Kawamoto T, Scharffetter-Kochanek K, Munzel T, Burkle A, Bachschmid MM and Daiber A. Manganese superoxide dismutase and aldehyde dehydrogenase deficiency increase mitochondrial oxidative stress and aggravate age-dependent vascular dysfunction. Cardiovasc Res 2008; 80: 280-289.
[20] van Bree SH, Gomez-Pinilla PJ, van de Bovenkamp FS, Di Giovangiulio M, Farro G, Nemethova A, Cailotto C, de Jonge WJ, Lee K, Ramirez-Molina C, Lugo D, Skynner MJ, Boeckxstaens GE and Matteoli G. Inhibition of spleen tyrosine kinase as treatment of postoperative ileus. Gut 2013; 62: 1581-1590.
[21] Endo M, Hori M, Ozaki H, Oikawa T and Hanawa T. Daikenchuto, a traditional Japanese herbal medicine, ameliorates postoperative ileus by anti-inflammatory action through nicotinic acetylcholine receptors. J Gastroenterol 2014; 49: 1026-1039.
[22] Schmittgen TD and Livak KJ. Analyzing real-time PCR data by the comparative C (T) method. Nat Protoc 2008; 3: 1101-1108.
[23] ZurNedden S, Eason R, Doney AS and Frenguelli BG. An ion-pair reversed-phase HPLC method for determination of fresh tissue adenine nucleotides avoiding freeze-thaw degradation of ATP. Anal Biochem 2009; 388: 108-114.
[24] Kehlet H and Holte K. Review of postoperative ileus. Am J Surg 2001; 182: 3S-10S.
[25] Boeckxstaens GE and de Jonge WJ. Neuroimmune mechanisms in postoperative ileus. Gut 2009; 58: 1300-1311.
[26] Seddon M, Looi YH and Shah AM. Oxidative stress and redox signalling in cardiac hypertrophy and heart failure. Heart 2007; 93: 903-907.
[27] Shen M, Wu RX, Zhao L, Li J, Guo HT, Fan R, Cui Y, Wang YM, Yue SQ and Pei JM. Resveratrol attenuates ischemia/reperfusion injury in neonatal cardiomyocytes and its underlying mechanism. PLoS One 2012; 7: e51223.

[28] Babu D, Leclercq G, Goossens V, Vanden Berghe T, Van Hamme E, Vandenabeele P and Lefebvre RA. Mitochondria and NADPH oxidases are the major sources of TNF-alpha/cycloheximide-induced oxidative stress in murine intestinal epithelial MODE-K cells. Cell Signal 2015; 27: 1141-1158.

[29] Naveenkumar C, Raghunandhakumar S, Asokkumar S and Devaki T. Baicalein abrogates reactive oxygen species (ROS)-mediated mitochondrial dysfunction during experimental pulmonary carcinogenesis in vivo. Basic Clin Pharmacol Toxicol 2013; 112: 270-281.

[30] Wendel M and Heller AR. Mitochondrial function and dysfunction in sepsis. Wien Med Wochenschr 2010; 160: 118-123.

[31] Kolling J, Scherer EB, Siebert C, Hansen F, Torres FV, Scaini G, Ferreira G, de Andrade RB, Goncalves CA, Streck EL, Wannmacher CM and Wyse AT. Homocysteine induces energy imbalance in rat skeletal muscle: is creatine a protector? Cell Biochem Funct 2013; 31: 575-584.

[32] Huang XP, Tan H, Chen BY and Deng CQ. Astragalus extract alleviates nerve injury after cerebral ischemia by improving energy metabolism and inhibiting apoptosis. Biol Pharm Bull 2012; 35: 449-454.

[33] Scheiner-Bobis G. The sodium pump. Its molecular properties and mechanics of ion transport. Eur J Biochem 2002; 269: 2424-2433.

[34] Kharbanda S, Saxena S, Yoshida K, Pandey P, Kaneki M, Wang Q, Cheng K, Chen YN, Campbell A, Sudha T, Yuan ZM, Narula J, Weichselbaum R, Nalin C and Kufe D. Translocation of SAPK/JNK to mitochondria and interaction with Bcl-x(L) in response to DNA damage. J Biol Chem 2000; 275: 322-327.

[35] Kaszuba-Zwoinska J, Ziomber A, Gil K, Bugajski A, Zaraska W and Thor P. Pulsating electromagnetic field induces apoptosis of rat's bowel Cajal's cells. Folia Med Cracov 2005; 46: 87-95.

[36] An S, Hishikawa Y, Liu J and Koji T. Lung injury after ischemia-reperfusion of small intestine in rats involves apoptosis of type II alveolar epithelial cells mediated by TNF-alpha and activation of Bid pathway. Apoptosis 2007; 12: 1989-2001.

[37] Abdelkader NF, Safar MM and Salem HA. Ursodeoxycholic Acid Ameliorates Apoptotic Cascade in the Rotenone Model of Parkinson's Disease: Modulation of Mitochondrial Perturbations. Mol Neurobiol 2014; [Epub ahead of print].

[38] Churchill EN, Disatnik MH and Mochly-Rosen D. Time-dependent and ethanol-induced cardiac protection from ischemia mediated by mitochondrial translocation of varepsilon PKC and activation of aldehyde dehydrogenase 2. J Mol Cell Cardiol 2009; 46: 278-284.

[39] Ohsawa I, Nishimaki K, Yasuda C, Kamino K and Ohta S. Deficiency in a mitochondrial aldehyde dehydrogenase increases vulnerability to oxidative stress in PC12 cells. J Neurochem 2003; 84: 1110-1117.

[40] Guo R, Zhong L and Ren J. Overexpression of aldehyde dehydrogenase-2 attenuates chronic alcohol exposure-induced apoptosis, change in Akt and Pimsignalling in liver. Clin Exp Pharmacol Physiol 2009; 36: 463-468.

[41] Ren J, Babcock SA, Li Q, Huff AF, Li SY and Doser TA. Aldehyde dehydrogenase-2 transgene ameliorates chronic alcohol ingestion-induced apoptosis in cerebral cortex. Toxicol Lett 2009; 187: 149-156.

[42] Gao Q, Wang HJ, Wang XM, Kang PF, Yu Y, Ye HW, Zhou H and Li ZH. Activation of ALDH2 with ethanol attenuates diabetes induced myocardial injury in rats. Food Chem Toxicol 2013; 56: 419-424.

[43] Wang HJ, Kang PF, Wu WJ, Tang Y, Pan QQ, Ye HW, Tang B, Li ZH and Gao Q. Changes in cardiac mitochondrial aldehyde dehydrogenase 2 activity in relation to oxidative stress and inflammatory injury in diabetic rats. Mol Med Rep 2013; 8: 686-690.